Tracer Diffusion of ^{59}Fe and ^{51}Cr in Fe-17 Wt Pct Cr-12 Wt Pct Ni Austenitic Alloy

R. A. PERKINS, R. A. PADGETT, JR., AND N. K. TUNALI

The volume and grain-boundary diffusion of ^{59}Fe and ^{51}Cr have been studied in an austenitic iron alloy containing 17 wt pct Cr and 12 wt pct Ni. The diffusivities in this alloy of these two tracers and ^{63}Ni are compared with their diffusivities in pure iron and in other austenitic stainless steels. For volume diffusion at any particular temperature in the present alloy, Cr is the most rapid while Ni is the slowest, and all three tracers diffuse slower than that reported for pure iron or for other austenitic stainless steels. For grain-boundary transport, Fe diffuses most rapidly above 850°C and Ni diffuses most rapidly below that temperature. The activation energies for both volume and grain-bounary diffusion obey the relationship $Q_{Ni} < Q_{Cr} < Q_{Fe}$.

THE atomic transport of iron, chromium, and nickel in the austenitic alloy Fe-17 wt pct Cr-12 wt pct Ni by both lattice and grain-boundary diffusion has been studied using radioactive tracer techniques. Results of the nickel investigation have been previously reported.[1] The results of the iron and chromium investigations are presented here, and the rates of diffusion of the three elements are compared. Parameters from the Arrhenius-type equation, $D = D_0 \exp[-Q/RT]$, for volume and grain-boundary diffusion of iron and chromium in pure gamma iron and in austenitic steels obtained by several investigators are summarized in Table I. A similar summary for nickel was made earlier.[1] The purpose of this investigation is to aid in the understanding of diffusion of major constituents in austenitic stainless steels, in particular in type 316 stainless steel.

Table I. Volume and Grain Boundary Diffusion Parameters for Fe-Base Alloys

	Q	D_0	Ref.
Cr Vol dif			
Fe	69.7	10.8	3
Fe-18 Cr-8 Ni	58.5	0.08	2
Fe-17 Cr-12 Ni	63.1	0.13	This study
Fe-20 Cr-25 Ni/Nb	58.8	0.19	4
Cr gb dif			
Fe-17 Cr-12 Ni	36.4	3.5×10^{-8}	This study
Fe-20 Cr-25 Ni/Nb	44.7	25×10^{-7}	4
Fe Vol dif			
Fe	67.8	1.05	5
Fe-18 Cr-8 Ni	67.1	0.58	6
Fe-17 Cr-12 Ni	66.8	0.36	This study
Fe-20 Cr-25 Ni/Nb	67.9	1.74	4
Fe gb dif			
Fe	40.0	1×10^{-7}	7
Fe-17 Cr-12 Ni	42.4	5.3×10^{-7}	This study
Fe-20 Cr-25 Ni/Nb	43.0	8×10^{-7}	4

EXPERIMENTAL

The specimens from the same bar of material previously used were prepared and polished in the manner previously described.[1] The radioactive ^{51}Cr and ^{59}Fe tracers were deposited onto the specimens either dropwise or by evaporation under a vacuum, and the specimens were sealed in quartz ampoules for the diffusion anneals.[1] Anneals for each isotope ranged from 600 to 1300°C at approximately 50°C intervals. Volume diffusion of the radioactive tracer was analyzed for specimens over the entire temperature range, and grain-boundary diffusion was analyzed for specimens from 600 to 1050°C. After its diffusion anneal, each specimen was serial sectioned to analyze the volume diffusion profile by lathe machining, hand grinding or sputtering depending upon the width of the volume diffusion zone.

The radiofrequency sputtering technique which allows the removal of very thin sections has been developed for serial sectioning which will permit the study of lattice diffusion at lower temperatures and more shallow penetrations.[8,9] The major components of the sputtering system are the sputtering module, the power supply and the vacuum system. A Materials Research Corporation Sputtering Module SM-8500 with a stainless steel cathode assembly has been modified to accept a $\frac{1}{2}$ in. diam specimen as the target cathode, and a rotating turntable with positions for 18 planchets was positioned to collect the material removed from the specimen. In addition, there is a bleed valve to leak argon into the sputtering chamber and a gas purification unit to clean the argon. The power supply is an MRC S-3005A 1 kw radiofrequency unit with a tuning network. The forward power meter on the power supply has been modified to indicate the forward current in μA instead of forward power to allow more precise power control.

The specimen size suitable for sputtering is $\frac{1}{2}$ in. in diam and approximately 3 mm thick. The specimen is placed into a threaded aluminum shield which will prevent removal of material from the sides of the specimen and define the area, approximately $\frac{3}{8}$ in. in diam, on the face of the specimen to be sputtered. The shield

R. A. PERKINS, formerly Presidential Intern in the Metals and Ceramics Division, Oak Ridge National Laboratory, is with Globe-Union, Inc., Milwaukee, Wis. 53201. R. A. PADGETT, Jr., is Technologist in the Metals and Ceramics Division, Oak Ridge National Laboratory, Oak Ridge, Tenn. 37830. N. K. TUNALI is with the Middle East Technical University, Ankara, Turkey.

Manuscript submitted January 10, 1973.

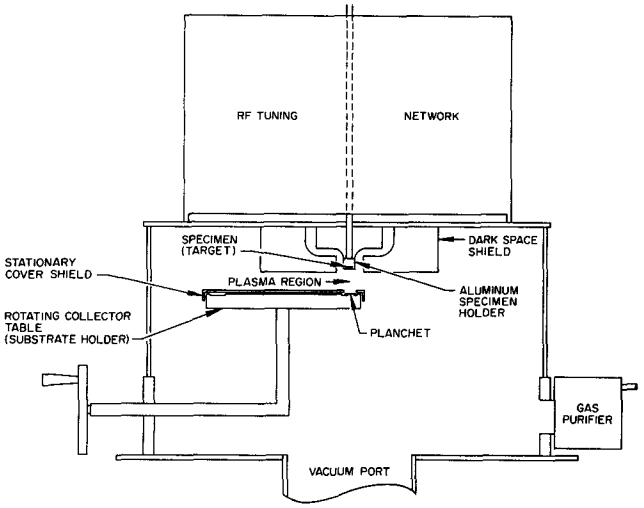

Fig. 1—Sputtering arrangement for serial sectioning of specimens.

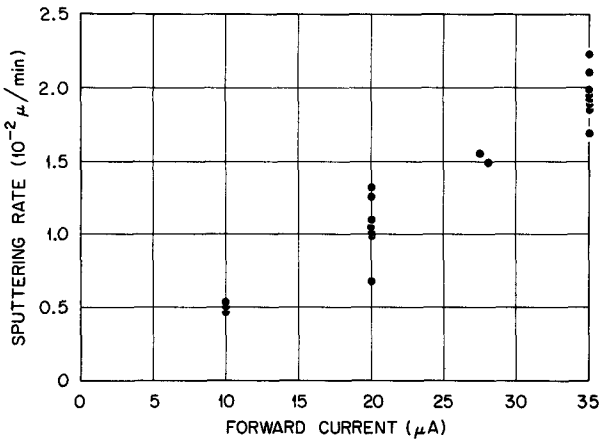

Fig. 2—Dependence of the rate of removal of material by sputtering as a function of the forward current setting applied in the system.

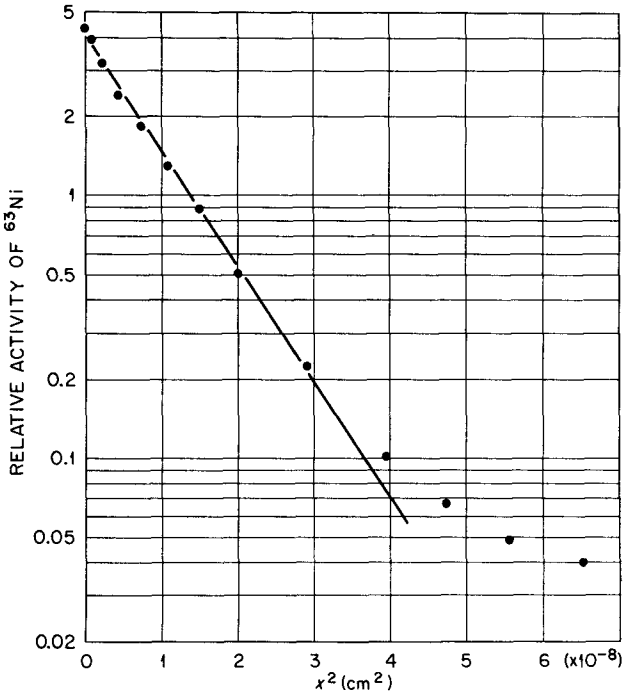

Fig. 3—Volume diffusion profile for ^{63}Ni diffusing into Fe-17 Cr-12 Ni at 750°C obtained by serial sectioning using the sputtering technique.

is then screwed onto a cathode post causing the specimen and shield to be the target during the sputtering run. The planchets which collect the sputtered material are $\frac{3}{4}$ in. in diam and are about 2 in. from the specimen. The arrangement in the vacuum chamber is shown in Fig. 1. As the sputtering continues, the turntable is rotated such that material for up to eighteen time segments can be collected on individual planchets allowing up to eighteen sections to be serial sectioned during a sputtering run. Approximately 10 pct of the material removed from the specimen is collected on the planchets. The section thicknesses were determined by measuring the specimen weight change during the sputtering run and determining the thickness of each section by relating the length of time material is collected on each planchet to the total weight removed. The resulting distribution of material on the planchets provides an excellent and uniform counting geometry for measuring the activity of tracer atoms on the planchets which is especially advantageous if α or β radiation is being measured because attenuation in the residual material from sectioning is important.

During the sputtering run the gas pressure and the forward current must be monitored. A dynamic gas pressure is maintained by leaking argon through the bleed valve and adjusting the gate to the diffusion pump until the desired pressure is maintained in the system. For the sputtering of quartz in a similar MRC apparatus, Blanco[10] has reported that the rate of deposition is independent of the gas pressure for argon atmospheres from 10 to 15 μ of mercury. The same pressure range was used in the present studies, and no dependence of the sputtering rate upon the gas pressure was observed. However, the importance of having a pure argon cover obtained by using the gas purification unit to clean the incoming gas was observed. If the argon was not cleaned, the initial sputtering rate was very rapid and gradually decreased until a steady rate was obtained. The forward current could be maintained within ± 1 μA which was suitable precision to avoid scatter in the results from power variations.

In the present investigation forward currents from 20 to 35 μA were used. The linear dependence of the sputtering rate upon the forward current is shown in Fig. 2. The rate varied from 0.005 μ per min at 20 μA to 0.02 μ per min at 35 μA. The sputtering rate at a particular current setting was fairly reproducible to within ±25 pct. When the argon is cleaned, a fairly constant sputtering rate was obtained as can be seen in Fig. 3 which is the ^{63}Ni concentration profile for lattice diffusion in the iron alloy at 750°C obtained by sputtering. The diffusion coefficients calculated from profiles obtained by sputtering are comparable with results from profiles from serial sectioning by grinding. Excellent results have been obtained for diffusion zones as shallow as 0.17 μ by sputtering with section thicknesses as thin as 0.015 μ yielding diffusion coefficients on the order of 10^{-18} sq cm per s. After sputtering runs at the higher current settings (≥ 35 μA) for very long times (>12 h) etching at the grain boundaries was observed. Therefore this technique would seem best suited for single crystal studies if penetrations greater than approximately 6 μ are desired. Some etching of the

grain boundaries would not be detrimental to the measurement of volume diffusion since the grain boundaries are concentration sinks and for large grains the etching would not greatly affect the tracer concentration measured on the planchets. Obviously, this technique could not be used to study grain boundary diffusion.

Specimens annealed at temperatures above 1105°C were sectioned by lathe techniques, specimens annealed from 700 to 1105°C by hand grinding or sputtering depending upon the length of the anneal and specimens annealed below 700°C by sputtering. If the specimen was to be sectioned on the lathe or by hand grinding, the sides of the specimen were turned down on the lathe to remove any edge effects. Each specimen sectioned by sputtering had approximately 2 mm rim of the specimen face shielded. After sputtering and prior to sectioning by hand grinding for the grain-boundary diffusion analysis, the diameter was reduced. After the volume diffusion zone was analysed, further sectioning of the specimens annealed at 1050°C or lower by grinding was continued to analyze the grain-boundary diffusion. The activity of ^{51}Cr or ^{59}Fe in the material removed by sectioning was measured using either a flat or well type 3 by 3 in. NaI(Tl) crystal in conjunction with a multichannel analyzer.

RESULTS

The method of analysis of the ^{51}Cr and ^{59}Fe concentration profiles obtained from sectioning and counting was identical to that previously reported.[1] The volume diffusion coefficients were evaluated from the slope of the logarithm of the tracer concentration plotted vs the square of the penetration distance at the near-surface region. The grain boundary diffusion coefficients were evaluated further into the sample from the slope of the logarithm of the tracer concentration plotted vs the penetration distance raised to the $\frac{6}{5}$ power using the Whipple solution.[11] The present results are listed in Tables II and III. The Arrhenius analysis for the volume diffusion yielded the following fit to the data:

$$D_v^{Fe} = (0.37 \pm 0.08) \exp[-(66{,}800 \pm 2800)/RT] \text{ cm}^2/\text{s} \quad [1]$$

and

$$D_v^{Cr} = (0.13 \pm 0.04) \exp[-(63{,}100 \pm 3000)/RT] \text{ cm}^2/\text{s}. \quad [2]$$

The Arrhenius analysis for the grain boundary results yielded

$$\delta D_{gb}^{Fe} = (5.3 \pm 1.4) \times 10^{-7} \exp[-(42{,}400 \pm 4100)/RT] \text{ cm}^3/\text{s} \quad [3]$$

and

$$\delta D_{gb}^{Cr} = (3.5 \pm 0.5) \times 10^{-8} \exp[-(36{,}000 \pm 2300)/RT] \text{ cm}^3/\text{s} \quad [4]$$

For completeness and to aid in comparing the diffusivities of the three isotopes, the results of the ^{63}Ni study[1] are included:

$$D_v^{Ni} = (8.8 \pm 1.7) \times 10^{-3} \exp[-(60{,}000 \pm 2600)/RT] \text{ cm}^2/\text{s} \quad [5]$$

Table II. Volume and Grain Boundary Diffusion for ^{59}Fe in Fe-17 wt pct Cr-12 wt pct Ni

Temperature (°C)	Time (s)	D_v (cm²/s)	δD_{gb} (cm³/s)
1297	1.728×10^5	1.57×10^{-10}	
1251	2.592×10^5	8.87×10^{-11}	
1198	6.048×10^5	3.39×10^{-11}	
1120	7.776×10^5	1.56×10^{-11}	
1033	4.176×10^5	1.69×10^{-12}	2.230×10^{-14}
1006	2.880×10^4	1.692×10^{-12}	
1000	2.700×10^4	1.731×10^{-12}	1.521×10^{-14}
948	1.728×10^5	4.051×10^{-13}	1.620×10^{-14}
948	6.840×10^5		2.138×10^{-14}
902	3.456×10^5		7.661×10^{-15}
900	5.184×10^5	1.304×10^{-13}	1.152×10^{-14}
848	1.1052×10^6		2.747×10^{-15}
800	1.3824×10^6	2.179×10^{-14}	6.348×10^{-16}
760	2.0736×10^6		1.148×10^{-15}
701	4.2336×10^6		2.100×10^{-16}
701	2.9376×10^6	1.534×10^{-16}	2.135×10^{-16}
661	2.3076×10^6	6.691×10^{-17}	
600	4.6656×10^6	9.169×10^{-18}	1.322×10^{-17}
597	4.9248×10^6		5.683×10^{-18}

Table III. Volume and Grain Boundary Diffusion for ^{51}Cr in Fe-17 wt pct Cr-12 wt pct Ni

Temperature (°C)	Time (s)	D_v (cm²/s)	δD_{gb} (cm³/s)
1295	1.728×10^5	2.38×10^{-10}	
1253	3.204×10^5	1.50×10^{-10}	
1205	6.048×10^5	5.34×10^{-11}	
1147	6.192×10^5	2.34×10^{-11}	
1104	5.796×10^5	8.72×10^{-12}	
1050	9.360×10^4	7.246×10^{-12}	2.771×10^{-14}
992	8.640×10^5	1.22×10^{-12}	2.049×10^{-14}
950	4.320×10^5	5.030×10^{-13}	8.247×10^{-15}
902	1.296×10^6		6.432×10^{-15}
902	4.320×10^5	4.010×10^{-13}	5.424×10^{-15}
850	1.1844×10^6	4.682×10^{-14}	3.346×10^{-15}
806	1.7280×10^6		1.518×10^{-15}
800	2.4192×10^6	3.085×10^{-14}	1.871×10^{-15}
749	3.0240×10^6	1.270×10^{-14}	6.126×10^{-16}
701	2.9376×10^6	3.018×10^{-16}	2.836×10^{-16}
699	2.5596×10^6		2.365×10^{-16}
652	3.6252×10^6	7.848×10^{-17}	6.482×10^{-17}
637	1.6986×10^6	1.59×10^{-16}	1.242×10^{-16}
603	4.3200×10^6	1.050×10^{-17}	1.375×10^{-17}
576	1.7280×10^6	1.776×10^{-17}	1.651×10^{-17}

and

$$\delta D_{gb}^{Ni} = (3.7 \pm 0.5) \times 10^{-9} \exp[-(32{,}000 \pm 1900)/RT] \text{ cm}^3/\text{s} \quad [6]$$

The width of the grain boundaries, δ, is included with the grain boundary diffusivities. The error limits indicate an 80 pct confidence in the calculated values using Student t statistics. The activation energies for volume diffusion increase by increments of approximately 3000 cal per mole from nickel to chromium to iron. The error limits for the activation energies overlap due to the closeness of the results. The activation energies for grain boundary diffusion vary by 4000 to 6000 cal per mole in the same order; again, the error limits overlap.

The Arrhenius plots for iron volume and grain-boundary diffusion are shown in Figs. 4 and 5 and are compared with the results obtained for iron in similar

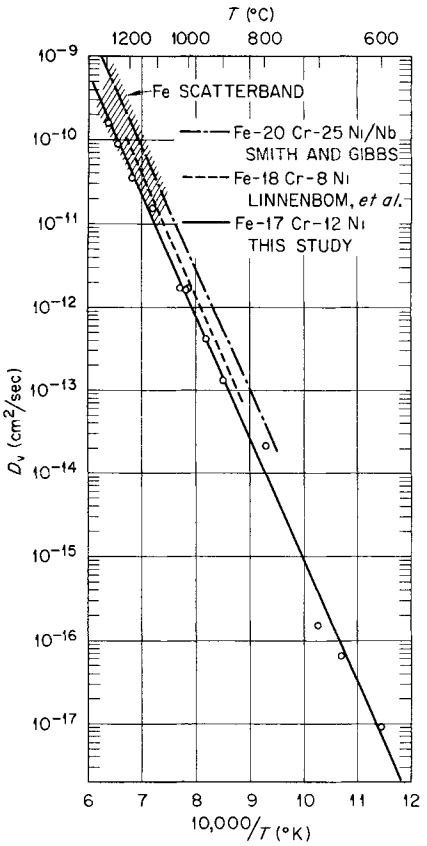

Fig. 4—Volume diffusion of ^{59}Fe.

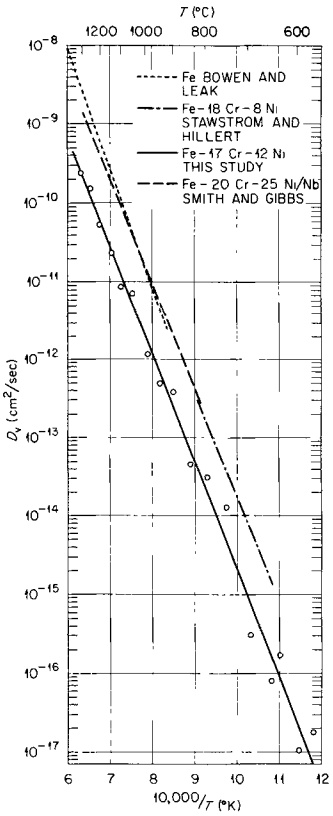

Fig. 6—Volume diffusion of ^{51}Cr.

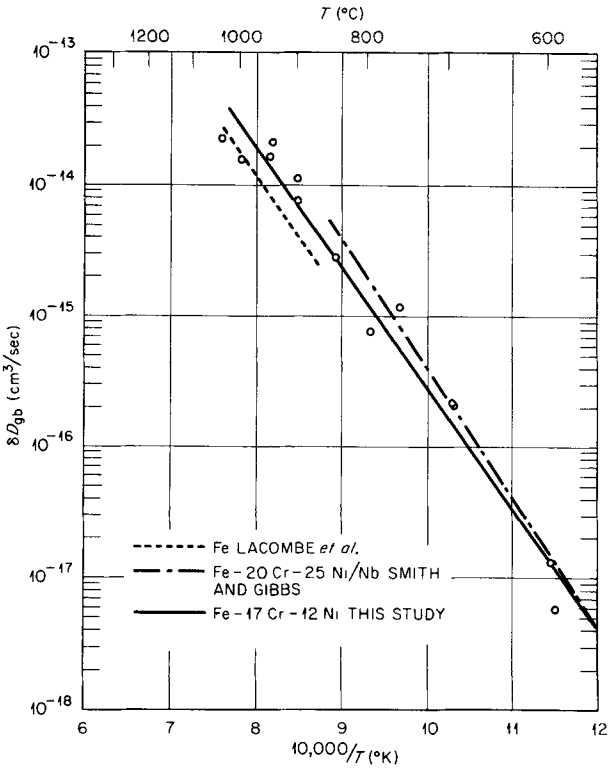

Fig. 5—Grain-boundary diffusion of ^{59}Fe.

systems. In Fig. 4 the scatterband for the results from the many studies of iron volume self-diffusion in gamma iron is shown along with the results from two austenitic steels. The rate of iron diffusion in the present system is shown to be somewhat smaller than in the two steels while the activation energies are nearly equal. In Fig. 5 the grain-boundary diffusion results for pure iron were obtained according to the Fisher analysis[12] while the other two investigations used the Whipple analysis.[11] Therefore the results for pure iron would be higher by a factor of 2 to 3 if analyzed by the Whipple analysis and would agree well with the other results shown.

The Arrhenius plot for chromium volume diffusion is shown in Fig. 6. From comparison with results from other studies, the rate of chromium volume diffusion in the present alloy is nearly an order of magnitude less than in pure iron or Fe-20 Cr-25 Ni/Nb. Also the activation energy varies a great deal for the three systems. The results for the grain-boundary diffusion of chromium are shown in Fig. 7 where the present data agree fairly well with the results for grain-boundary diffusion of chromium in Fe-20 Cr-25 Ni/Nb although the activation energies are quite different.

In Figs. 8 and 9 the results for iron, chromium and nickel are shown for volume diffusion and grain-boundary diffusion, respectively, in the present system. The volume diffusion rate of chromium is the fastest, while that of nickel is the slowest in the temperature range studied. The activation energy of nickel is the lowest and of iron the highest. The rates of grain-boundary diffusion for the three elements are nearly the same over most of the temperature range although the differences become greater at the highest and lowest temperatures. At approximately 850°C the diffusivities of all three elements along grain boundaries are equal while above 850°C iron diffuses most rapidly and below 850°C nickel diffuses most rapidly. The activation energy increases from the grain-boundary diffusion of nickel to chromium to iron as was observed for volume diffusion.

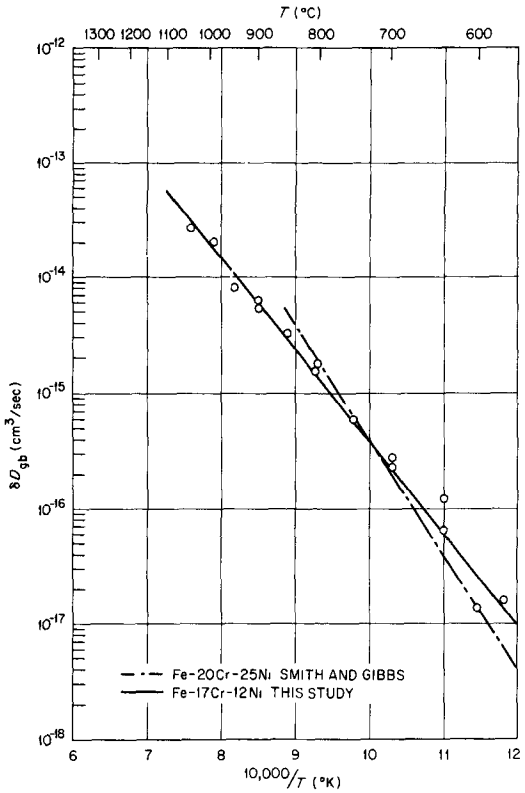

Fig. 7—Grain-boundary diffusion of ^{51}Cr.

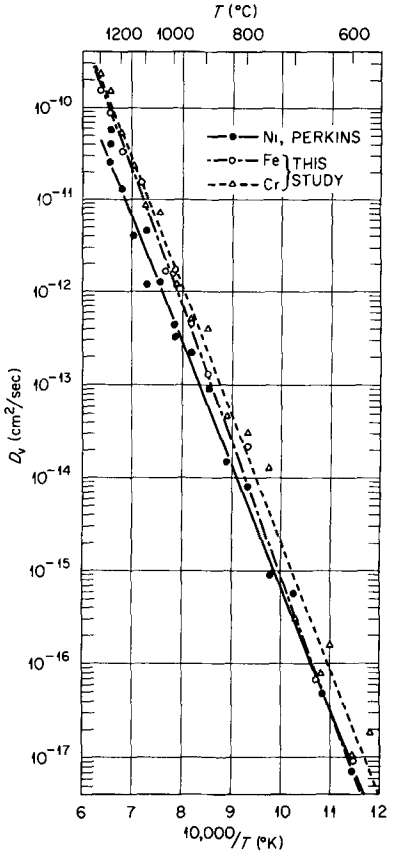

Fig. 8—Volume diffusion in Fe-17 Cr-12 Ni.

DISCUSSION

The volume diffusion of iron, chromium, and nickel[1] in the present system is consistently lower than in pure iron or in austenitic stainless steels although the iron results are more compatible with other studies than the other two elements. From Table I the diffusion parameters from the results of Linnenbom *et al.*[6] for the diffusion of iron in 18-8 stainless steel are nearly the same as for iron in the present alloy, and the activation energies in all four materials are nearly identical. Smith and Gibbs[4,13] have conducted an investigation analogous to the present study in Fe-20 Cr-25 Ni/Nb austenitic stainless steel over a narrower temperature range. Their results indicated that the volume diffusivities of chromium and nickel are appreciably greater than that of iron and that the grain-boundary diffusivities of the three elements are nearly identical. Although there are large compositional differences between their system and the alloy used in the present investigation, the most significant difference is the change in the nickel content. The addition of nickel to the austenitic iron lattice has been concluded to decrease the interatomic bond strength of the lattice.[14] This decrease in bond strength would cause an increase in the diffusivity of species in the lattice. Therefore, volume diffusion in the present system might be expected to be slower than in Fe-20 Cr-25 Ni/Nb steel. However, if the relation between the "average group number" of an alloy and the bond strength in the alloy as indicated by Smith and Gibbs[13] were extended to include the present system, no difference between the diffusivity in pure iron, this alloy or the stainless steels would be predicted. The addition of chromium to the iron lattice has been concluded to increase the interatomic bond

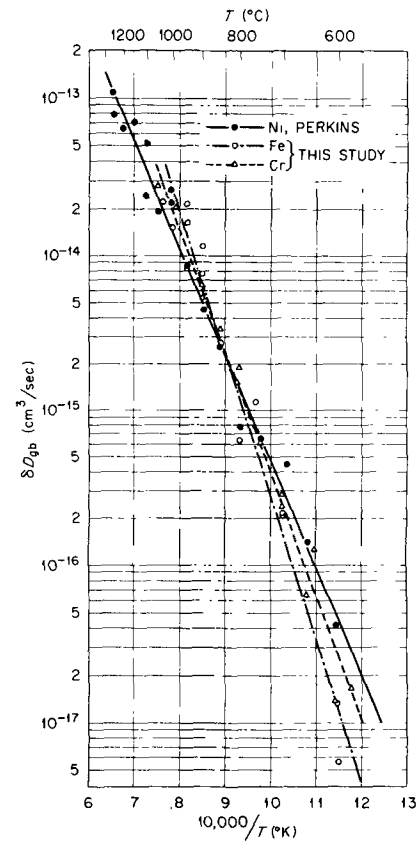

Fig. 9—Grain-boundary diffusion in Fe-17 Cr-12 Ni.

strength in the austenitic lattice,[15] which would decrease the rate of diffusion. This decrease might account for the fact that volume diffusion in the present system is lower than in pure iron while further nickel additions seem to increase the rate. The data for the diffusion of chromium in 18-8 stainless steel[2] would oppose this trend. However, the latter data were obtained indirectly and might not be as reliable as direct measurements over the same temperature range as that study.

Due to the similar ionic radii of iron, chromium, and nickel, chromium and nickel will occupy sites on the face-centered cubic iron lattice, and all three elements will diffuse via vacancies. Because all three elements are present in large amounts, bonding energies between the individual atoms and vacancies are expected to be negligible.[16] However, if the various species have different jump frequencies, correlation effects can become significant. In this case the volume diffusivity of a particular species, i, is given by

$$D_v = f_i a_0^2 \gamma_i \exp\left[\frac{\Delta S_f + \Delta S_{m,i}}{R}\right] \exp\left[\frac{-\Delta H_f - \Delta H_{m,i}}{RT}\right] \quad [7]$$

where a_0 is the lattice constant, f_i is the correlation factor of the species i, γ_i is the vibrational frequency of the species i, ΔS_f and ΔH_f are the entropy and enthalpy of vacancy formation and $\Delta S_{m,i}$ and $\Delta H_{m,i}$ are the entropy and enthalpy of a vacancy i-atom exchange. The parameters which are capable of changing for each species are f_i, $\Delta S_{m,i}$ and $\Delta H_{m,i}$; γ_i is assumed to be essentially the same for all three elements. Zener[18] has shown that the entropy of diffusion should be directly proportional to the enthalpy, this relationship has been substantiated for fcc systems.[19] The frequency factor

$$D_0 = f_i a_0^2 \gamma \exp\left[\frac{\Delta S_f + \Delta S_{m,i}}{R}\right] \quad [8]$$

should, therefore, increase as the activation energy increases if f_i is constant.

Because the jump frequency is given by

$$w_i = \gamma \exp\left(\frac{-\Delta G_{m,i}}{RT}\right) \quad [9]$$

the jump frequency for each species will increase as the activation energy decreases because ΔG_f is constant; therefore, $w_{Ni} > w_{Cr} > w_{Fe}$. For alloys which contain 10 pct atom fraction or more of impurity, Manning has proposed that all sites in the crystal have the same vacancy binding energy. An average jump frequency is then defined as[17]

$$W = N_1 w_1 + N_2 w_2 + N_3 w_3 \ldots N_n w_n \quad [10]$$

where N_n and w_n are the mole fraction and jump frequency of the n-th species in the lattice, respectively. The correlation factor for each species is then given by[17]

$$f_i = 7.151W/(2w_i + 7.151W) \quad [11]$$

for an fcc lattice. Therefore, because w_i increases as the activation energy decreases, the correlation factor will decrease as the activation energy decreases. This yields $f_{Ni} < f_{Cr} < f_{Fe}$, thus causing D_0 to decrease as Q decreases even beyond the change caused by ΔS. Approximate values for f_i are calculated to be: $f_{Ni} \sim 0.5$; $f_{Cr} \sim 0.7$; and $f_{Fe} \sim 1.0$. Therefore, the correlation effect could contribute to the low diffusivity observed for nickel.

The activation energies for grain-boundary diffusion of the three elements follow the same trend as for the volume diffusion. Because the grain-boundary diffusion is related to the volume diffusion, this trend is not unexpected. The grain-boundary diffusivities of the three elements are nearly equal at 850°C. Above 850°C iron diffuses most rapidly and nickel is the slowest while below 850°C the relative rates are reversed. The results for iron agree well with results from other systems while rather large differences are observed for chromium and nickel. The grain-boundary diffusion analysis is compounded by the possibility of impurities and minor constituents segregating to the grain boundaries and by carbide formation. These effects could greatly affect the rate of diffusion down the grain boundaries. Large differences were observed for activation energies for chromium and nickel grain-boundary diffusion in the various systems considered, which might be attributable to the impurity and alloying elements present. The various effects which need to be considered when determining the volume and grain-boundary diffusion coefficients from the same specimen have been previously discussed.[1]

CONCLUSIONS

1) The volume diffusion coefficients for ^{59}Fe and ^{51}Cr in Fe-17 Cr-12 Ni have been determined from 600 to 1300°C and are represented by Eqs. [1] and [2], respectively.

2) The grain-boundary diffusion coefficients for ^{59}Fe and ^{51}Cr in Fe-17 Cr-12 Ni have been determined to be represented by Eqs. [3] and [4], respectively.

3) The activation energies for both volume and grain-boundary diffusion have been observed to increase from nickel to chromium to iron.

4) Correlation effects might help account for the low diffusivity of nickel in the present system.

REFERENCES

1. R. A. Perkins: *Met. Trans.*, 1973, vol. 4, pp. 1665-69.
2. C. Stawström and M. Hillert: *J. Iron Steel Inst.*, 1969, vol. 207, pp. 77-85.
3. A. W. Bowen and G. M. Leak: *Met. Trans.*, 1970, vol. 1, pp. 1695-1700.
4. A. F. Smith and G. B. Gibbs: *Met. Sci. J.*, 1969, vol. 3, pp. 93-94.
5. B. Sparke, D. W. James, and G. M. Leak: *J. Iron Steel Inst.*, 1965, vol. 203, pp. 152-53.
6. V. Linnenbom, M. Tetenbaum, and C. Cheek: *J. Appl. Phys.*, 1955, vol. 26, pp. 932-36.
7. P. Lacombe, P. Guiraldenq, and C. Leymone: *Radioisotopes in the Physical Sciences and Industry*, pp. 179-92, 1962.
8. D. Gupta and R. T. C. Tsui: *Appl. Phys. Letters*, 1970, vol. 17, pp. 294-97.
9. D. Gupta: *Phys. Rev.*, 1973, vol. 7, pp. 586-94.
10. B. L. Blanco: AEC Research and Development Report MLM-1850, Mound Laboratory, U. S. Government Contract No. AT-33-1-GEN-53, 1971.
11. R. T. P. Whipple: *Phil. Mag.*, 1954, vol. 45, p. 1225.
12. J. C. Fisher: *J. Appl. Phys.*, 1951, vol. 22, pp. 74-77.
13. A. F. Smith and G. B. Gibbs: *Met. Sci. J.*, 1968, vol. 2, pp. 47-50.
14. I. E. Sulayev, A. N. Kurasov, N. A. Karpov, and A. V. Rabinovick: *Russ. Met.*, 1970, vol. 4, pp. 150-53.
15. M. A. Krishtal: *Diffusion Processes in Iron Alloys*, 1963, p. 140, Israel Program for Scientific Translations, Keter Press, Jerusalem.
16. J. R. Manning: *Phys. Rev. B*, 1971, vol. 4, pp. 1111-21.
17. J. R. Manning: *Phys. Rev.*, 1959, vol. 116, pp. 819-27.
18. C. Zener: *Imperfections in Nearly Perfect Crystals*, p. 289, W. Shockley, ed., J. Wiley, New York, 1952.
19. P. G. Shewmon: *Diffusion in Solids*, p. 66, McGraw-Hill, New York, 1963.